Rationalisation of anomalous pseudo-contact shifts and their solvent dependence in a series of C_3-symmetric lanthanide complexes

Michele Vonci,[1] Kevin Mason,[2] Elizaveta A. Suturina,[3] Andrew T. Frawley,[2] Steven G. Worswick,[3] Ilya Kuprov,[3,*] David Parker,[2,*] Eric J. L. McInnes[1,*] and Nicholas F. Chilton[1,*]

[1] School of Chemistry, The University of Manchester, Oxford Road, Manchester M13 9PL, U.K.

[2] Department of Chemistry, Durham University, South Road, Durham, DH1 3LE , U.K.

[3] School of Chemistry, The University of Southampton, Highfield, Southampton SO17 1BJ, U.K.

ABSTRACT

Bleaney's long-standing theory of magnetic anisotropy has been employed with some success for many decades to explain paramagnetic NMR pseudo-contact shifts, and has been the subject of many subsequent approximations. Here, we present a detailed experimental and theoretical investigation accounting for the anomalous solvent dependence of NMR shifts for a series of lanthanide(III) complexes, namely [LnL^1] (Ln = Eu, Tb, Dy, Ho, Er, Tm, and Yb; L^1: 1,4,7-tris[(6-carboxypyridin-2-yl)methyl]-1,4,7-triazacyclononane), taking into account the effect of subtle ligand flexibility on the electronic structure. We show that the anisotropy of the room temperature magnetic susceptibility tensor, which in turn affects the sign and magnitude of the pseudo-contact chemical shift, is extremely sensitive to minimal structural changes in the first coordination sphere of L^1. We show that DFT structural optimisations do not give accurate structural models, as assessed by the experimental chemical shifts, and thus we determine a magneto-structural

correlation and employ this to evaluate the accurate solution structure for each [LnL^1]. This approach allows us to explain the counter-intuitive pseudo-contact shift behaviour, as well as a striking solvent dependence. These results have important consequences for the analysis and design of novel magnetic resonance shift and optical emission probes that are sensitive to the local solution environment.

INTRODUCTION

Complexes of lanthanide (Ln) ions are widely used in biochemical and medical applications of NMR spectroscopy including, for example, magnetic resonance imaging and structural and functional study of biological systems.[1-6] A cornerstone of this area has been the interpretation of chemical shift data *via* Bleaney's theory of magnetic anisotropy.[7,8] This theory states that, for remote nuclei – where the Fermi contact term δ_c is vanishingly small, as discussed by others[9] – the paramagnetic chemical shift is dominated by the pseudo-contact (dipolar) shift (δ_{pc}) and can be simply related to the crystal field (CF), the geometry, and a factor that relates to the identity of the specific Ln ion. For an axially symmetric complex, δ_{pc} is approximated by Equation 1. Here, θ and r are the polar coordinates of the NMR active nucleus with respect to the principal axes of the magnetic susceptibility tensor χ, B_2^0 is the second rank axial CF parameter of the Hamiltonian Equation 2 (where $\hat{O}_k^q$ are the Steven's operator equivalents and $\langle J\|k\|J\rangle$ are the operator equivalent factors) and $C_J = g_J^2 J(J+1)(2J-1)(2J+3)\langle J\|k=2\|J\rangle$ is Bleaney's constant. Since C_J is a function of the total angular momentum J and the Landé factor g_J, its value depends only on the electronic configuration of the lanthanide ion.

$$\delta_{pc} = -\frac{C_J\beta^2}{30(kT)^2}\left(\frac{3\cos^2\theta-1}{r^3}\right)B_2^0 \qquad (1)$$

$$\widehat{H} = \sum_{k,q} B_k^q \langle J \| k \| J \rangle \hat{O}_k^q \qquad (2)$$

The crucial assumptions made by Bleaney were: (i) that the total CF splitting is << *kT*, and (ii) that *J* is a good quantum number. If these assumptions hold, only second order terms of temperature (*T*) are required to accurately describe the magnetic susceptibility. Furthermore, it is often assumed that the axial CF parameter and the geometric part $\frac{3\cos^2\theta - 1}{r^3}$ do not vary across an isostructural series of complexes, in which case the relative order of δ_{pc} for a given nucleus in an isostructural series of lanthanide complexes should follow C_J, or in other words, there should be a linear relationship between the experimentally determined values of δ_{pc} and C_J (C_J values for some Ln^{III} = Tb -158; Dy -181; Ho -71.2; Er +58.8; Tm +95.3; and Yb +39.2).[7] While this simplistic description has been proven correct in many cases,[10,11] it has been found to be invalid in some recent works,[12,13,14] failing to reproduce even the trends in experimental shifts across isostructural series of Ln complexes. Discrepancies are often attributed to the many approximations given above, without specifying the main source. In certain cases, the "culprit" seems clear, as in the case reported by Piguet and co-workers where a sudden structural variation across the Ln series leads to abrupt change in the value of B_2^0.[15]

A relevant example, reported by some of us, concerns behaviour in the [LnL^1] family.[12] This set of complexes constitutes the archetypal 9-coordinate system in C_3 symmetry, with the smallest ligand field splitting known for a lanthanide coordination complex, (Ln = Eu, Tb, Dy, Ho, Er, Tm and Yb; L^1 = 1,4,7-tris[(6-carboxypyridin-2-yl)methyl]-1,4,7-triazacyclononane, Figure 1, left). In this family, the Ln ions adopt a tricapped trigonal prismatic {N_6O_3} coordination geometry, *via* an N3-macrocycle (providing the axial N-donors) with pendant pyridyl arms (providing the capping equatorial N-donors), and carboxylate substituents on the pyridyl groups (providing the axial O-

donors). For these complexes, despite the CF being relatively weak, the relative order and magnitude of the δ_{pc} of the three unique pyridyl ^{1}H nuclei (pyH$^{3\text{-}5}$) do not correlate with the value of Bleaney's constant. Based on C_J alone and assuming a constant value of B_2^0, the expected order of the pseudo-contact shifts for the pyridyl protons should be Dy < Tb < Ho < Yb < Er < Tm, while experimentally, the order is found to be Tb < Ho < Er < Yb < Dy < Tm. In this series and two closely related isostructural series based on triazacyclononane, it was shown, with the aid of two/three nuclei plots devised by Reuben/Geraldes, that resonances from the pyridyl protons located some 5.4 to 6.3 Å from the metal centre were not subject to any significant contact shift.[12]

Here, we provide a detailed explanation of the origin of the peculiar paramagnetic NMR behaviour of [LnL^1], including the origin of a new and significant solvent dependence (D_2O, MeOD and d_6-DMSO). We demonstrate how the delicately balanced CF provided by the L^1 ligand renders the sense of magnetic anisotropy, i.e. easy axis ($\chi_{\parallel} > \chi_{\perp}$) or easy plane ($\chi_{\parallel} < \chi_{\perp}$), extremely responsive to seemingly trivial geometric changes in the first coordination sphere, ultimately controlling the sign and magnitude of the pseudo-contact paramagnetic NMR shift. This is not the first time that the tricapped trigonal prismatic geometry has been implicated in anomalous pseudo-contact shifts,[16-18] however, we rationalise the origins of such effects for the first time in terms of the underlying electronic structure of the lanthanide complexes.

RESULTS AND DISCUSSION

We focus on the NMR shifts of the three pyridyl ^{1}H nuclei (pyH3-5), which are quite distant from the lanthanide ion (Figure 1, left) and hence their paramagnetic shifts should be dominated by the pseudo-contact term; this is justified by Reuben/Geraldes plots in ref. 12 showing that the contact contribution is very small, and experimentally validated here (see below and Figure S7). We first consider [DyL^1] which shows a striking departure from the simple assumptions given above, having (i) a pseudo-contact shift for pyH3-5 of the same sign (positive) as the late Ln complexes [TmL^1] and [YbL^1] despite Dy^{III} having opposite sign of C_J from Tm^{III} and Yb^{III} (Figure 1, center); and (ii) a large solvent dependence of δ_{pc} (Figure 1, right), where even the order of the pyH3-5 resonances changes (Figure S1). We note that this solvent dependence is not due to the change in diamagnetic shift, as these are negligible for the [YL^1] complex (Table S1) to which all our paramagnetic shift values are referenced.

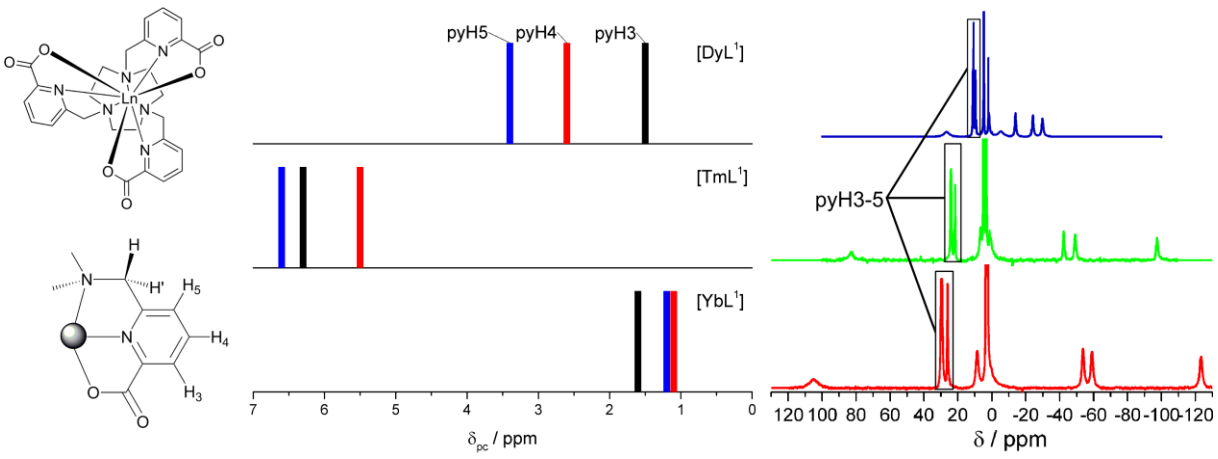

Figure 1. (*Left*) Structure of [LnL^1] and assignment of the three pyridyl (py) H atoms. (*Centre*) Schematic representation of the δ_{pc}values for thr pyH3-5 resonances of [DyL^1], [TmL^1], and

[YbL^1] (in D_2O, 298 K). (*Right*) NMR spectra (absolute shifts, δ) of [DyL^1] in D_2O (*blue*), MeOD (*green*), and d_6-DMSO (*red*) solution (298 K).

In order to understand the relationship between the electronic structure, magnetic anisotropy and pseudo-contact NMR shifts for [DyL^1], we have employed a fully *ab initio* calculation of the paramagnetic shift, similar to that employed recently for [Yb(DTMA)]$^{3+}$.[19] In this approach we approximate the solution structure by optimisation with density functional theory (DFT, see Supporting Information), starting from the closest crystal structure,[20,21] in the presence of a continuum solvent model while imposing the C_3 symmetry experimentally observed in the solution NMR.[12] Initially we employed the M06 functional[22] with the SMD solvent model.[23] The electronic structure and resulting room temperature magnetic susceptibility tensor were then determined for this pseudo-solution structure using complete active space self-consistent field spin orbit (CASSCF-SO) calculations (see Supporting Information).

The theoretical δ_{pc} were subsequently calculated using Equation 3,[7,8] where $\chi_{\parallel} - \chi_{av}$ is the anisotropy of the molar magnetic susceptibility in cm^3 mol^{-1} ($\chi_{av} = \frac{(\chi_{\parallel}+2\chi_{\perp})}{3}$), N_A is Avogadro's number, and r is the Ln···H distance in metres. The δ_{pc} calculated with this method (M06/SMD, Table 1) are catastrophically in error compared to the experiment, even having the incorrect sign for all three protons. Therefore, we tried different approaches: (i) using the same functional but different continuum solvent model (PCM,[24] still using the parameters for water), and (ii) a different functional (BP86) with the same solvent model. These gave completely different results for the calculated pseudo-contact shifts (Table 1).

$$\delta_{pc} = \frac{\chi_{\parallel} - \chi_{av}}{2N_A}\left(\frac{3\cos^2\theta - 1}{r^3}\right) \qquad (3)$$

Table 1. Calculated and experimental pseudo-contact shifts for [DyL^1] pyridyl H atoms in D_2O at 298 K.

	Experimental[a] (ppm)	**M06/SMD (ppm)**	**M06/PCM (ppm)**	**BP86/SMD (ppm)**
pyH3	2.9	-19.3	7.8	-33.3
pyH4	2.4	-15.3	6.0	-24.8
pyH5	1.7	-17.7	6.6	-25.4

[a] Diamagnetic contributions, determined experimentally from [YL^1] (Table S1) were removed from the experimental shifts.

We were curious why such a small change in the DFT method could lead to such drastic changes in the calculated δ_{pc} given that both solvent models and both functionals are widely employed in the literature. Comparing the three optimised structures we observe no appreciable differences in the 1,4,7-triazacyclononane backbone, and only very subtle changes in the orientations of the carboxypyridyl rings (Figure S2). The calculated root mean square deviation (RMSD)[25,26] between each pair of optimised structures are 0.09 (M06/SMD *vs.* M06/PCM), 0.14 (M06/SMD *vs.* BP86/SMD) and 0.07 Å (M06/PCM *vs.* BP86/SMD), highlighting the minimal differences. The similarity of the structures has an important consequence in the analysis of the NMR properties of [DyL^1]. There are two contributions to the pseudo-contact shift (Equation 3): the structural part $\left(\frac{3\cos^2\theta - 1}{r^3}\right)$ and the magnetic anisotropy term ($\chi_{\parallel} - \chi_{av}$). For each proton, the structural part shows little difference across the three optimised structures (< 10% variation, Table S2) and importantly, does not change sign. Hence, it must be changes in the magnetic anisotropy term

causing the large changes in the calculated δ_{pc}. Therefore, the electronic structure of [DyL^1] must be very sensitive to the coordination geometry such that seemingly trivial structural variations, such as those described above, can induce large changes (including sign) in the magnetic anisotropy. This is not only important when assessing DFT methods for providing reliable structural models, but also reflects the intrinsic sensitivity of the electronic structure of [DyL^1] – and by implication the whole [LnL^1] family – to minimal structural distortions.

A plausible origin for this extreme sensitivity may be explained intuitively with point charge CF theory in terms of the axial and equatorial contribution of the ligands.[27-29] The first coordination sphere possesses three sets of three symmetry-equivalent donor atoms: the N-atoms from the 1,4,7-triazacyclononane backbone (N_{ax}) that lie in axial positions (polar angle from the C_3 axis $\theta \sim 142°$), the N-atoms from the pyridyl ring (N_{eq}) that lie in equatorial positions ($\theta \sim 90°$), and the O-atoms from the carboxylate residues that are in axial positions ($\theta \sim 50°$). From the very simplistic viewpoint of point charge CF theory, donor atoms switch between axial and equatorial nature at the magic angle of $\theta \sim 55°$ (or equivalently, 125°).[30] In [DyL^1] the two sets of N donor atoms (N_{ax} and N_{eq}) give contributions of similar magnitude but opposite sign to B_2^0, and roughly cancel each other out. However, the O-donor atoms lie close to the magic angle and hence we may expect some sensitivity of the magnetic anisotropy under minimal variation of their positions. This is quite different to the situation reported by Binnemans and Görller-Walrand,[31] where a small or zero value of B_2^0 for tricapped trigonal prismatic complexes results from accidental cancellation, when the polar angle for both sets of equivalent axial donors is 45°.

To quantify the effect of minor structural variations in [DyL^1], we conducted a systematic *ab initio* study of the dependence of the magnetic susceptibility tensor on the polar angle θ for each set of

donor atoms. Using the M06/SMD optimised structure as a starting point we altered θ for each set of donor atoms individually (whilst the other two sets were fixed), and allowed the rest of the ligand (i.e. excluding donor atoms) to relax whist maintaining C_3 symmetry. We then calculated the room temperature anisotropy of the magnetic susceptibility tensor with CASSCF-SO (Figure 2). We observe that an increase of *ca.* 2 degrees in θ for either the O- or the N_{ax}-atoms is sufficient to change the sign of the magnetic anisotropy $\chi_{\parallel} - \chi_{av}$. In contrast, small angular distortions at the N_{eq}-atoms, i.e. the pyridyl nitrogen atoms, do not invert the sign of the magnetic anisotropy.

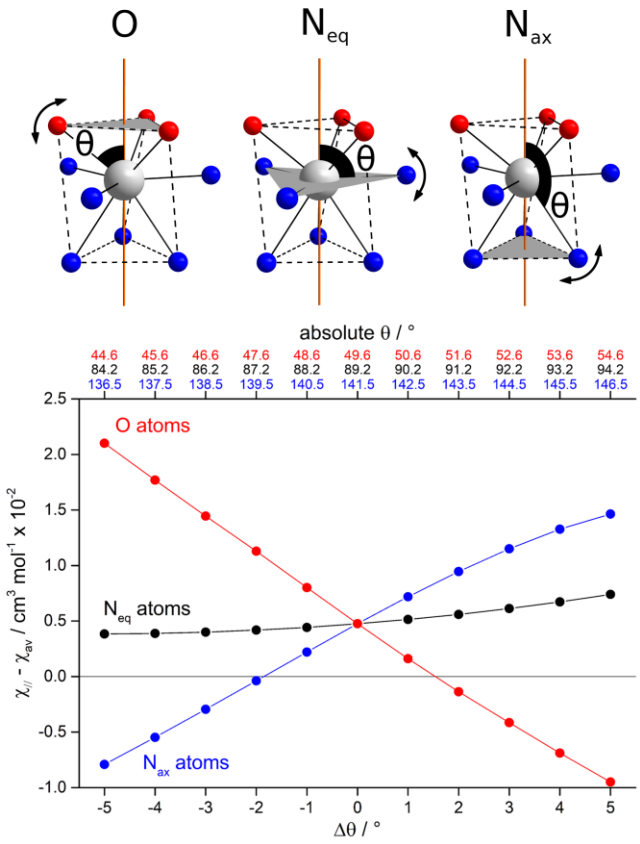

Figure 2. (Top) Schematic of the variation of polar angles (θ) for O, N_{eq}, and N_{ax} donor atoms in [DyL^1]. (Bottom) Calculated anisotropy of the room temperature magnetic susceptibility resulting from distortions. $\Delta\theta$ is the deviation in the M06/SMD optimised structure.

In light of the similar effect for the O and N_{ax}-atoms , we compared the relative DFT energies of the partially optimised structures for these distortions (Table S3, Figure S3). These data clearly show that movement of the O-atoms is much more facile than movement of the N_{ax}-atoms within the relatively rigid 9-N_3 ring, and that a variation of $\Delta\theta = \pm 2°$ (i.e. sufficient to change the sign of the magnetic anisotropy) for the O-donors is within kT at 298 K. Thus, we conclude that the structural distortion responsible of the variation of the susceptibility tensor, and hence δ_{pc}, is most likely to be associated with the movement of the axial O donor atoms.

Inspection of the partially optimised structures for different polar angles for the O-atoms shows that the main differences are in the rigid rotation of the pyridyl rings (Figure S4): these can be parameterised by two torsion angles $C_A N_B C_C C_D$ (labelled β) and $N_B C_C C_D N_E$ (labelled α). The variation of α is three times larger than that of β (Figure S5), suggesting that changes in θ can be adequately mapped through variation of α alone. Indeed, CASSCF-SO calculations of the magnetic susceptibility tensor as a function of α alone agree well with its dependence on θ (Figure S6); hence we adopt α as the sole variable to study the effects of structural variations.

In order to understand the origin of the change in room temperature magnetic anisotropy under such a small structural change, we examined the electronic structure of the ground J = 15/2 multiplet as a function of α (Dy^{III} has a $^6H_{15/2}$ ground state in the Russell-Saunders formalism). The calculated electronic structure of the reference M06/SMD geometry (α = 40.4°, which gives a polar angle of θ = 49.6° for the O donors) gives two low-lying Kramer's doublets, very close in energy (*ca.* 11 cm^{-1}, Figure 3), which have characteristic g-tensors that are easy axis ($g_{||} > g_{\perp}$) and easy plane ($g_{||} < g_{\perp}$) for the ground and first excited doublet, respectively (Figure 3 and Table S4).

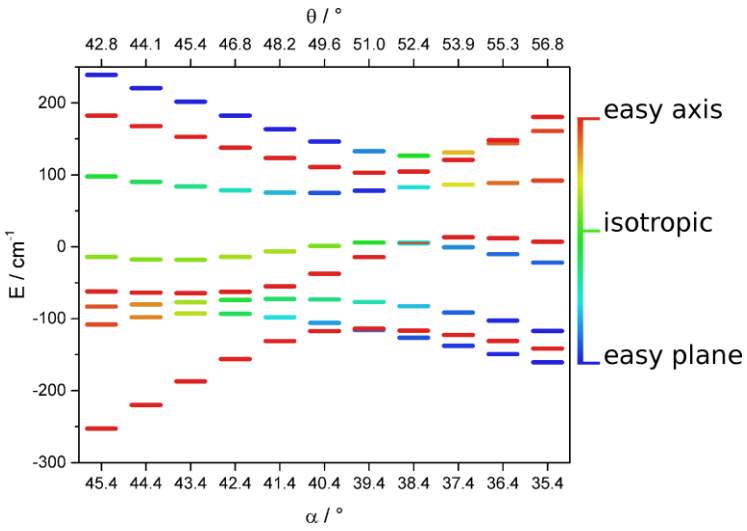

Figure 3. CASSCF-SO calculated energy levels of the J = 15/2 ground multiplet of Dy^{III} in [DyL^1] as a function of α (and corresponding O-donor polar angle θ). The data for α = 40.4° (θ = 49.6°) correspond to the DFT optimised reference geometry (M06/SMD). The barycentre of each multiplet is set to zero. The magnetic anisotropy of the Kramers doublets is visualised as red for an easy axis doublet ($g_{||} > g_{\perp}$), green for an isotropic doublet ($g_{||} = g_{\perp}$) and blue for an easy plane doublet ($g_{||} < g_{\perp}$). Kramers doublets between perfectly easy axis and isotropic will appear orange/yellow, and those between fully easy plane and isotropic will appear light blue/green.

Upon decreasing α by only 1° from the reference geometry, hence increasing θ to a value closer to the magic angle, the two lowest doublets swap order, resulting in an easy plane ground state and an easy axis first excited state (Figure 3 and Table S4). This change coincides with the change in sign of the calculated room temperature magnetic susceptibility anisotropy, although this necessarily results from contributions due to all Boltzmann-populated excited doublets at 298 K. Furthermore, decreasing α consolidates this trend with the two lowest Kramer's doublets progressively moving further apart and an increased easy plane character of the ground doublet; the opposite trend is observed for increasing α from the reference geometry. Interestingly, the

optimised reference geometry is very close to the minimum overall CF splitting of the J = 15/2 multiplet (Figure 3), corresponding to a CF which does not favour any particular magnetic states and thus gives a near-isotropic magnetic susceptibility. In terms of the CF Hamiltonian Equation 2, we observe that only the second rank axial term B_2^0 changes sign as a function of α and that it has by far the largest variation of all the CF parameters (Figure 4, Table S5; only $B_2^0, B_4^{0,\pm3}, B_6^{0,\pm3,\pm6}$ terms are allowed in C_3 symmetry). Therefore, it is clear why an anomalous trend is observed for the pseudo-contact shifts of [LnL^1]: B_2^0 is very sensitive to very minor changes in geometry in this ligand system and cannot be assumed to be a constant.

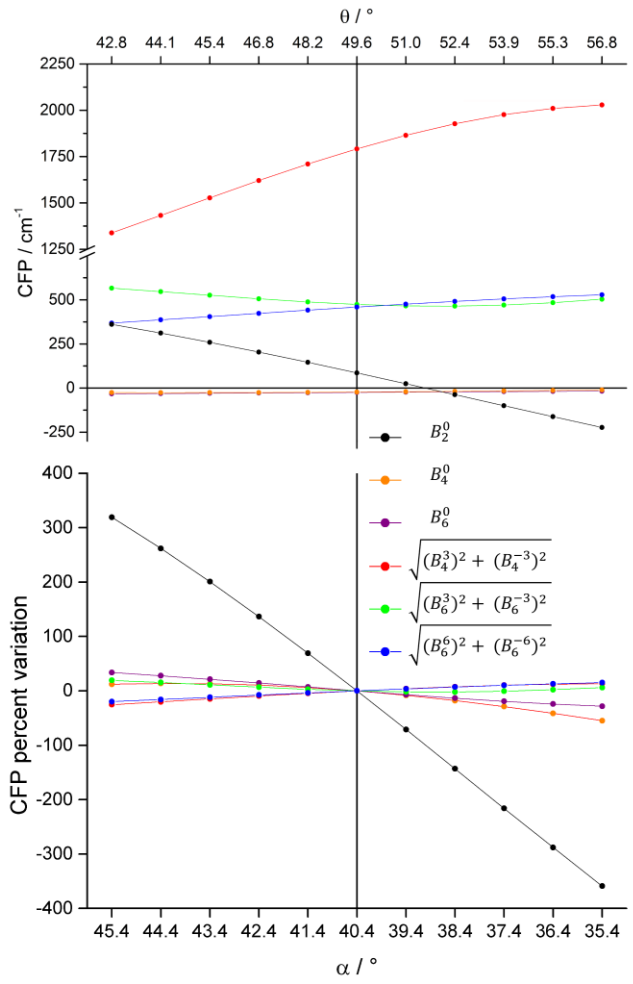

Figure 4. (Top) *Ab initio* CF parameters as a function of α (and corresponding polar angle at the O-donors, θ) for [DyL^1]. (Bottom) Percentage variation of *ab initio* CF parameters with respect to the reference geometry. For the B_k^q and B_k^{-q} with $q \neq 0$, we give $\sqrt{(B_k^q)^2 + (B_k^{-q})^2}$ to remove the arbitrary choice of *xy* reference axes. The data for α = 40.4° correspond to the reference DFT optimised structure in H_2O (M06/SMD).

Our analysis shows the extreme sensitivity of the magnetic anisotropy, even at room temperature, of [DyL^1] towards tiny variations in ligand torsion angles, on the order of a few degrees. As a consequence, any attempt to reproduce the solution phase pseudo-contact NMR shifts in this

family of complexes using DFT-optimised structures is a lottery, depending on the choice of lanthanide, DFT functional and solvent model. However, by developing a magneto-structural correlation of the magnetic susceptibility tensor with the torsion angle α, we are able to empirically determine the solution structure of [DyL^1] in this solvent system (D_2O); in order to match the experimental magnetic susceptibility anisotropy $\chi_{\parallel} - \chi_{av}$ and thus δ_{pc}, we determine that $\alpha = 38.8°$ (Figures 5 and S7).

We now turn to the solvent dependence of the pseudo-contact shifts in [DyL^1]. Experimentally, we find that the measured δ_{pc} for pyH3-5 become more positive, and have a larger spread, on moving from D_2O to MeOD to d_6-DMSO (Figures 1 and S1). Unsurprisingly, given the results above, optimised structures obtained with M06/SMD for MeOH and DMSO solvent parameterisations do not lead to δ_{pc} values that agree with experiment (Table S6). In order to generalise our approach across all three solvents, and hence determine the solution structures, we adopt a few sensible approximations. Firstly, we have tested and can show that the dependence of the magnetic anisotropy on the polar angle of the O-donors (θ, mapped through systematic variation of α) is practically identical when starting from DFT optimised geometries with MeOD, d_6-DMSO and D_2O solvent parameterizations (Figure S8). Secondly, we have tested and observe that the structural part in Equation 3 varies very little across the D_2O, MeOD and d_6-DMSO optimised structures ($\leq$ 3%, Table S7), or for variation in α (within a sensible range) for a given solvent ($\leq$ 3%, Table S8). Hence, we hypothesise that the experimentally observed solvent dependence of δ_{pc} is due to changes in the anisotropy of the magnetic susceptibility.

Under the assumption that for [DyL^1] the contact contribution is negligible and hence the paramagnetic shift is dominated by δ_{pc},[13] we can find the latter by plotting the experimental δ_{pc}

of protons as a function of the structural part of Equation 3: the slope then gives the magnetic susceptibility anisotropy ($\chi_{\parallel} - \chi_{av}$) for [DyL^1] in each solvent system (Figure S7). Then, we can correlate these against the calculated angular dependence of $\chi_{\parallel} - \chi_{av}$ to determine the structure of [DyL^1] in each solvent (Figure 5). We determine α = 38.8, 37.9 and 37.5° for D_2O, MeOD and d_6-DMSO, respectively, corresponding to polar angles for the O-donors of θ = 52.0, 53.3 and 53.8°, respectively. Hence, our results indicate that the O-donor atoms become more axial as the polarity, and H-bonding ability, of the solvent increases.[32] This suggests that solvating water molecules 'tug' on the oxygen atoms at the "open face" of the molecule more strongly than MeOD and d_6-DMSO.

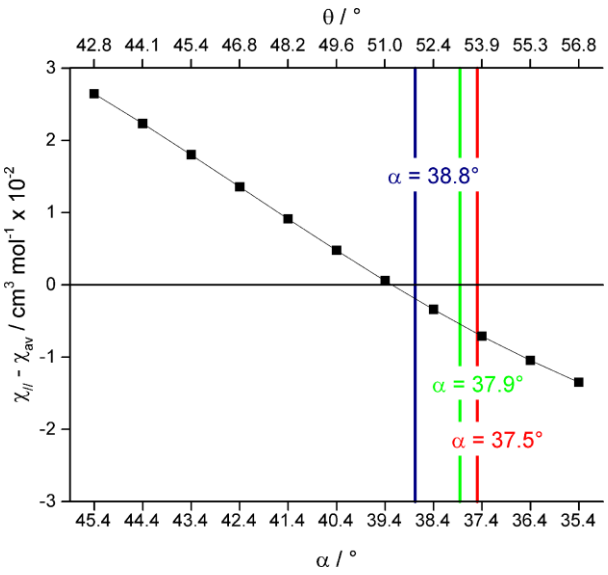

Figure 5. Determination of α and corresponding θ at which the CASSCF-SO calculated anisotropy of the susceptibility tensor $\chi_{\parallel} - \chi_{av}$ (black squares) matches the experimental value extracted from NMR data in D_2O (blue line), MeOD (green line), d_6-DMSO (red line) for [DyL^1]. Reference geometry calculated at the M06/SMD level for H_2O.

The role that tiny structural distortions have on the magnetic anisotropy of [DyL^1] is further exemplified by the variable temperature NMR signal of pyH3-5 in MeOD in the 205-300 K range (Figure S9); the experimental anisotropy $\chi_{\parallel} - \chi_{av}$ becomes more negative as the temperature diminishes. By interpolating the *ab initio* susceptibility anisotropy dependence on α, it is possible to construct the surface $S(\alpha,T)$ mapping the variation of the magnetic anisotropy with α and T (Figure S10). Plotting the experimental values of the magnetic anisotropy on the surface $S(\alpha,T)$ we observe that the anisotropy changes less than it should as a function of temperature if α remained constant; therefore, there must be a small structural relaxation with temperature on the order of $\Delta\alpha$ ~ 0.2° to account for the experimental results.

Independent confirmation of the solvent effect on the electronic structure is possible with the complementary technique of luminescence spectroscopy for [DyL^1] and [EuL^1] in H_2O, MeOH, and DMSO solutions. The $^4F_{9/2} \rightarrow {}^6H_{15/2}$ emission lines of [DyL^1] show slight differences in fine structure due to the modified CF splitting in different solvents (Figure S11), however, the small CF splitting and low resolution of the spectra prevents any reliable assignment. On the other hand, the solvent dependence of the emission lines for [EuL^1] is very informative. These spectra feature the usual $^5D_0 \rightarrow {}^7F_{0,1,2,3,4}$ emission bands in the 570-720 nm region (Figure S12), and the fine structure due to the CF splitting of each of the ^7F_n spin-orbit multiplets clearly differs between solvents. The $^5D_0 \rightarrow {}^7F_1$ transition is particularly diagnostic, because in trigonal symmetry the $^7F_1$ multiplet splits into a doublet (M_J = ±1) and a singlet (M_J = 0), the ordering and separation of which depending only on the second rank axial CF parameter B_2^0; the doubly degenerate level being higher in energy for negative values of B_2^0.[31] The luminescence spectra for this transition shows the $^7F_1$ splitting increasing as H_2O < MeOH < DMSO (Figure 6); circularly polarized luminescence does not increase the resolution of these spectra (Figure S13). Fitting the emission

lines with a two component Gaussian model gives the expected 1:2 ratio (Table S9), and shows that the sign of B_2^0 is negative in all three solvents (Table S10). In the same way that we have fit α to the experimental magnetic anisotropy of [DyL^1], we can fit α to the experimental CF splitting of the $^7F_1$ multiplet observed by luminescence spectroscopy for [EuL^1] (Figure S14). The solvent-dependent trend in α, and correspondingly in θ, agrees with that of [DyL^1], with increasingly larger values of θ going from H_2O to MeOH to DMSO (Figures S14 and S15). Thus, the independent techniques of NMR and luminescence spectroscopy for two different lanthanides reveal the same structural sensitivity towards solvent.

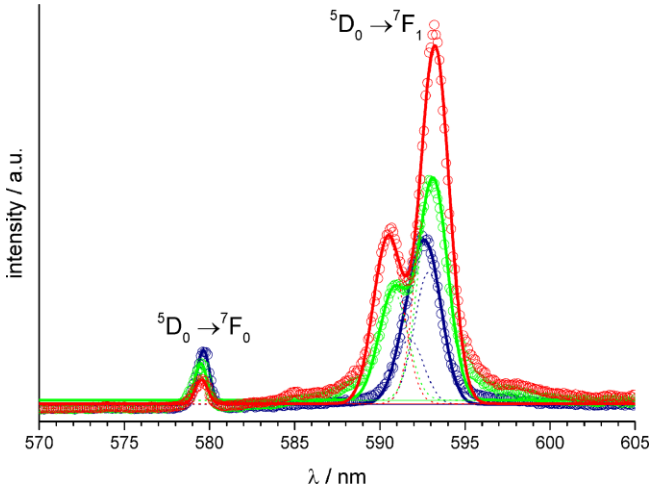

Figure 6. Luminescence spectrum of [EuL^1] in H_2O (*blue*), MeOH (*green*), and DMSO (*red*) in the region of the $^5D_0 \rightarrow {}^7F_0$ and $^5D_0 \rightarrow {}^7F_1$ emission lines (λ_{exc} = 272 nm, 295 K, 30 μM complex). Experimental data (open circles), deconvolution of the bands with two Gaussians (dotted lines), and fitted spectra (solid lines). Due to the poor resolution of the spectra in H_2O and MeOH, the Gaussian fitting in these solvents was performed by fixing the linewidth of the individual contributions to that of the better resolved spectrum in DMSO.

For the remaining late lanthanide complexes of the series, namely [TbL^1], [HoL^1], [TmL^1], and [YbL^1], the *ab initio* calculated room temperature anisotropy of the susceptibility tensor shows the same extreme sensitivity to small variations of the polar angle θ of the O-donor atoms that we observe for [DyL^1], implying a subsequent sensitivity of the δ_{pc} values (Figure S16). Such behaviour suggests that the hypersensitivity of the electronic structure towards geometrical changes is consistent across the entire [LnL^1] series. However, the overall paramagnetic shifts for [EuL^1] and [ErL^1] are very small in these three solvents and cannot be approximated with total confidence as being solely due to the pseudo-contact term;[13] this issue is a consequence of their small magnetic moments and minimal magnetic anisotropy, respectively. The same is true for [TbL^1] and [HoL^1] in D_2O, where the susceptibility is also very close to isotropic.

In all the other cases ([TmL^1] and [YbL^1] in each solvent, [TbL^1] and [HoL^1] in MeOD and d_6-DMSO), the δ_{pc} have a linear correlation with the structural part of Equation 3, showing that the pseudo-contact term is indeed dominant, allowing extraction of the experimental susceptibility anisotropy (Figure S7).[13] Variation of solvent for these complexes shows that δ_{pc} of pyH3-5 has the same strong dependence as observed for [DyL^1] (Figure S17), including even a change in sign of the δ_{pc} values for [TmL^1] and [YbL^1] moving from D_2O to MeOD, which implies that the susceptibility anisotropy switches from easy plane in D_2O to easy axis in MeOD and d_6-DMSO. This in contrast with [DyL^1], which shows easy plane anisotropy in all solvents (Figure S7). The same analysis for [TbL^1] and [HoL^1] in MeOD and d_6-DMSO reveals an easy plane anisotropy, similarly to [DyL^1]. In all cases, the fitted values of α show the same trend as the [DyL^1] and [EuL^1] analogues: α decreases, and as a consequence θ for the O-donor atoms increases, going from D_2O to MeOD to d_6-DMSO (Figure S16). The fitted angles, and hence the structure, vary depending on the lanthanide and solvent, meaning that the CF is not the same across the series.

The changes in CF across the [LnL^1] series are very subtle and yet crucial in order to understand the experimental pseudo-contact shifts. Rather than just a small change in magnitude of the CF along the series, like the ~ ±15% change reported by Bertini *et al.* across a series of Ln-bound calbindin protein samples,[10] we observe that the B_2^0 CF term can in fact change sign in response to a change of solvent, even when that solvent is not coordinated to the metal. Such hypersensitivity of the electronic structure for lanthanide chelates may be more common than currently surmised, and a careful study of anomalous experimental results may provide further examples of delicately balanced CFs, such as those defined herein.

CONCLUSION

Our magneto-structural correlation allowed us to explain the anomalous trend in D_2O of [DyL^1] having the same sign of δ_{pc} as [TmL^1] and [YbL^1] as well as the variation of δ_{pc} for [LnL^1] (Ln = Tb, Dy, Ho, Tm, Yb) across solvents, including the change in sign of δ_{pc} from D_2O to MeOD for [TmL^1] and [YbL^1]. We have shown that the deviations from simple interpretations using Bleaney's theory for [LnL^1] are due to the very peculiar nature of the tricapped trigonal prismatic ligand L^1, resulting in hypersensitivity of the electronic structure to minimal variations in the position of the O donor atoms. In this case, the structural part of Bleaney's equation (Equation 1) is approximately constant and it is the second rank axial CF parameter B_2^0 that can vary dramatically, including changing sign, upon minimal variation of the coordination geometry.

Thus, we conclude that B_2^0 cannot be considered a constant in this series of complexes. We have shown that significant variations in the NMR pseudo-contact shifts in different solvents are due to small structural variations, likely owing to solvent polarity and/or hydrogen bonding propensity, and have independently confirmed this with luminescence spectroscopy. These results have

important consequences for the design of magnetic resonance shift agents and responsive optical probes. The ease of modulation of the size and sign of B_2^0 associated with this ligand type could be exploited in developing probes that respond to small physicochemical perturbations, e.g. from changes in the local environment, such as medium polarity.

ACKNOWLEDGEMENTS

We thank the EPSRC for funding (EP/N007034/1 and EP/N006909/1); NFC thanks the Ramsay Memorial Trust for a Research Fellowship.

SUPPORTING INFORMATION

Paramagnetic NMR shift data for [Ln.L[1]], DFT structural examination, CASSCF-SO results, extraction of magnetic anisotropy, luminescence data and fitting, computational methods, NMR methods, optical methods.

AUTHOR INFORMATION

Corresponding Authors

*i.kuprov@soton.ac.uk

*david.parker@durham.ac.uk

*eric.mcinnes@manchester.ac.uk

*nicholas.chilton@manchester.ac.uk

Notes

The authors declare no competing financial interest

REFERENCES

(1) Piguet, C.; Geraldes, C. F. G. C. Paramagnetic NMR Lanthanide Induced Shifts for Extracting Solution Structures. In *Handbook on the Physics and Chemistry of Rare Earths, Volume 33*; 2003; pp 353–463.

(2) Faulkner, S.; Blackburn, O. A. The Chemistry of Lanthanide MRI Contrast Agents. In *The Chemistry of Molecular Imaging*; Long, N., Wong, W.-T., Eds.; John Wiley & Sons, Inc: Hoboken, NJ, 2014; pp 179–197.

(3) Su, X.-C.; Liang, H.; Loscha, K. V.; Otting, G. *J. Am. Chem. Soc.* **2009**, *131*, 10352–10353.

(4) Brath, U.; Swamy, S. I.; Veiga, A. X.; Tung, C.-C.; Van Petegem, F.; Erdélyi, M. *J. Am. Chem. Soc.* **2015**, *137*, 11391–11398.

(5) Chen, W.-N.; Nitsche, C.; Pilla, K. B.; Graham, B.; Huber, T.; Klein, C. D.; Otting, G. *J. Am. Chem. Soc.* **2016**, *138*, 4539–4546.

(6) Takano, Y.; Tashita, R.; Suzuki, M.; Nagase, S.; Imahori, H.; Akasaka, T. *J. Am. Chem. Soc.* **2016**, *138*, 8000–8006.

(7) Bleaney, B. *J. Magn. Reson.* **1972**, *8*, 91–100.

(8) Bleaney, B.; Dobson, C. M.; Levine, B. A.; Martin, R. B.; Williams, R. J. P.; Xavier, A. V. *J. Chem. Soc. Chem. Commun.* **1972**, *13*, 791–793.

(9) Reilley, C. N.; Good, B. W.; Desreux, J. F. *Anal. Chem.* **1975**, *47*, 2110–2116.

(10) Bertini, I.; Janik, M. B. L.; Lee, Y.-M.; Luchinat, C.; Rosato, A. *J. Am. Chem. Soc.* **2001**, *123*, 4181–4188.

(11) Desreux, J. F.; Reilley, C. N. *J. Am. Chem. Soc.* **1976**, *98*, 2105–2109.

(12) Funk, A. M.; Finney, K. N. A.; Harvey, P.; Kenwright, A. M.; Neil, E. R.; Rogers, N. J.; Kanthi Senanayake, P.; Parker, D. *Chem. Sci.* **2015**, *6*, 1655–1662.

(13) Castro, G.; Regueiro-Figueroa, M.; Esteban-Gómez, D.; Pérez-Lourido, P.; Platas-Iglesias, C.; Valencia, L. *Inorg. Chem.* **2016**, *55*, 3490–3497.

(14) Keizers, P. H. J.; Saragliadis, A.; Hiruma, Y; Overhand, M; Ubbink, M. *J. Am. Chem. Soc.* **2008**, *130*, 14802–14812.

(15) Ouali, N.; Bocquet, B.; Rigault, S.; Morgantini, P.-Y.; Weber, J.; Piguet, C. *Inorg. Chem.* **2002**, *41*, 1436–1445.

(16) Reuben, J. *J. Magn. Reson.* **1982**, *50*, 233–236.

(17) Peters, J. A. *J. Magn. Reson.* **1986**, *68*, 240–251.

(18) Mironov, V. S.; Galyametdinov, Y. G.; Ceulemans, A.; Görller-Walrand, C.; Binnemans, K. *J. Chem. Phys.* **2002**, *116*, 4673–4685.

(19) Blackburn, O. A.; Chilton, N. F.; Keller, K.; Tait, C. E.; Myers, W. K.; McInnes, E. J. L.; Kenwright, A. M.; Beer, P. D.; Timmel, C. R.; Faulkner, S. *Angew. Chem. Int. Ed.* **2015**, *54*, 10783–10786.

(20) Gateau, C.; Mazzanti, M.; Pécaut, J.; Dunand, F. A.; Helm, L. *Dalton Trans.* **2003**, *0*, 2428–2433.

(21) Nocton, G.; Nonat, A.; Gateau, C.; Mazzanti, M. *Helv. Chim. Acta* **2009**, *92*, 2257–2273.

(22) Zhao, Y.; Truhlar, D. G. *Theor. Chem. Acc.* **2008**, *120*, 215–241.

(23) Marenich, A. V.; Cramer, C. J.; Truhlar, D. G. *J. Phys. Chem. B* **2009**, *113*, 6378–6396.

(24) Scalmani, G.; Frisch, M. J. *J. Chem. Phys.* **2010**, *132*, 114110.

(25) Walker, M. W.; Shao, L.; Volz, R. A. *CVGIP Image Underst.* **1991**, *54*, 358–367.

(26) Kabsch, W. *Acta Crystallogr. Sect. A* **1976**, *32*, 922–923.

(27) Rinehart, J. D.; Long, J. R. *Chem. Sci.* **2011**, *2*, 2078–2085.

(28) Sievers, J. *Zeitschrift für Phys. B Condens. Matter* **1982**, *45*, 289–296.

(29) Chilton, N. F.; Collison, D.; McInnes, E. J. L.; Winpenny, R. E. P.; Soncini, A. *Nat. Commun.* **2013**, *4*, 2551.

(30) Sorace, L.; Benelli, C.; Gatteschi, D. *Chem. Soc. Rev.* **2011**, *40*, 3092–3104.

(31) Binnemans, K.; Görller-Walrand, C. *Chem. Phys. Lett.* **1995**, *245*, 75–78.

(32) Reichardt, C.; Welton, T. Empirical Parameters of Solvent Polarity. In *Solvents and Solvent Effects in Organic Chemistry*; Reichardt, C., Welton, T., Eds.; Wiley-VCH Verlag GmbH & Co. KGaA: Weinheim, Germany, 2010; pp 425–508.

TOC